WMO STATEMENT ON THE STATUS OF THE GLOBAL CLIMATE IN 1993

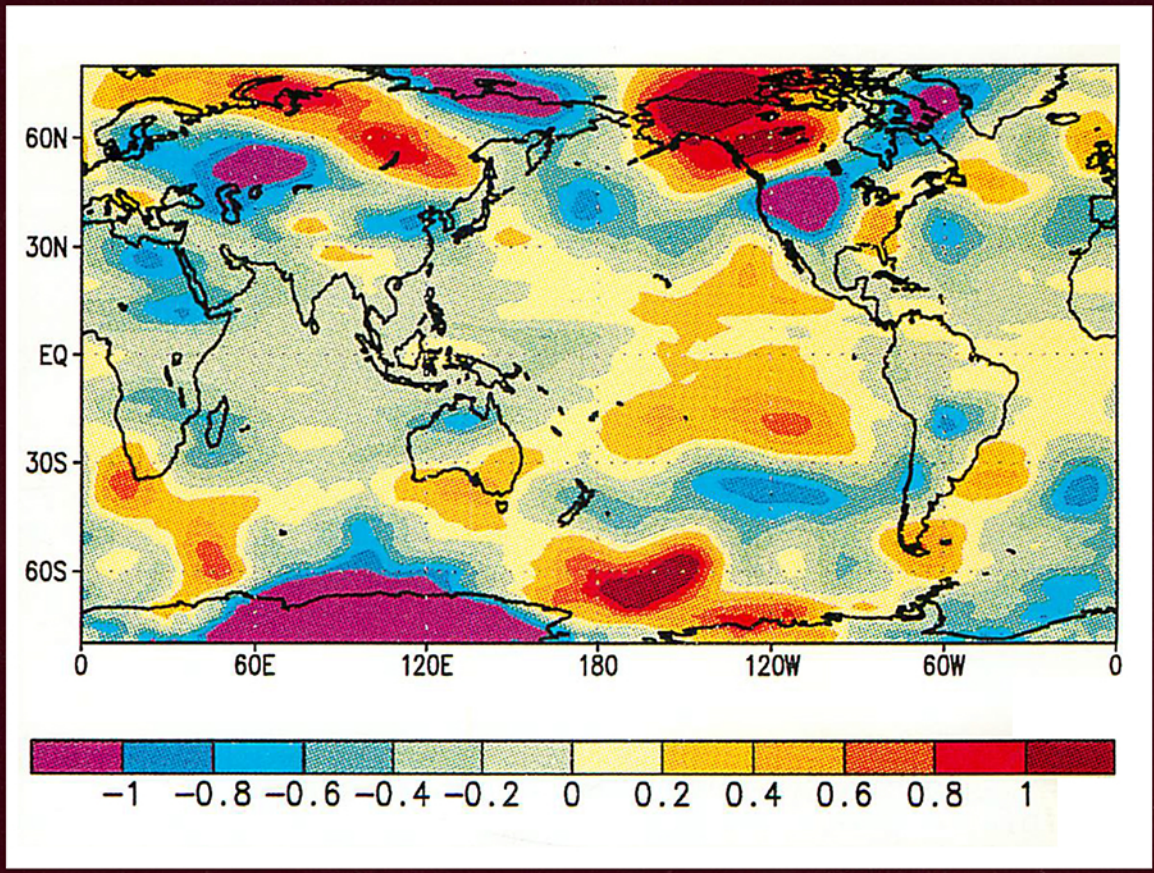

World Meteorological Organization
WMO-No. 809

Cover: Mean Tropspheric temperature anomalies (1979–1993 base period) derived from the Microwave Sounding Unit (MSU) on NOAA polar orbiting satellites.
Source: Data-John Christy, U of Alabama, Huntsville; Analysis-Climate Analysis Center/NMC.

WMO STATEMENT ON THE STATUS OF THE GLOBAL CLIMATE IN 1993

World
Meteorological
Organization

Geneva - Switzerland
1994

WMO-No. 809

WMO-No. 809
1994, World Meteorological Organization

ISBN 92-63-10809-9

NOTE

PREFACE

It has long been recognized that the climate system varies naturally on all time scales from hundreds of millions of years to a few years, as revealed by paleo-climatic data and instrumented observations. In recent years, there has been a realization of, and a growing concern about the impact of human activities on climate, particularly the effect of steadily increasing concentrations of greenhouse gases in the atmosphere. The latest scientific projections indicate an increase of the global mean temperature of one degree Celsius above 1990 levels by the year 2025 and a 3°C warming by the end of the next century. Such a short-term change in the climate would be unprecedented in the known climate history of the world and could lead to consequential changes in the economic and social well-being of the world's population. It could also seriously hamper efforts to promote and implement sustainable development practices.

The heightened concern about an imminent global warming has engendered a world-wide interest in shorter term year-to-year and even month to month fluctuations in the global climate system with the prime interest being the detection of a human-induced climate change signal. Detecting a climate change signal would not only confirm scientific predictions, but it would also accelerate efforts to mitigate and adapt to climate change. Routine monitoring of regional and global climate on shorter time scales has therefore become a preoccupation in many countries of the world.

Much of our knowledge on climate comes from global scientific and technical programmes coordinated by WMO. The Organization's mandate is to coordinate and facilitate world-wide cooperation in making and exchanging standardized and quality-controlled meteorological, hydrological and geophysical observations as well as their analysis, understanding and interpretation. WMO is sensitive and responsive to the changing global needs for meteorological and hydrological support to an ever-widening spectrum of human activities.

WMO, working with UNEP, is responsible for the periodic assessments of climate change issued by the Intergovernmental Panel on Climate Change, and for the routine publication of the Climate System Monitoring Monthly Bulletin and the biennial reviews of the Global Climate System. The latter two publications are outputs from the Climate System Monitoring project of the World Climate Data and Monitoring Programme (WCDMP). In June 1993, the 45th session of the Executive Council of WMO decided

that greater efforts were needed to promote the WMO role as a provider of credible scientific information on climate and its variability and requested that arrangements be made for the regular wide distribution, starting in 1994, of WMO statements on the status of the global climate. In response to this decision, this first statement is provided through the Climate Change Detection project of the WCDMP.

This statement is a summary of the information provided by the Climate Analysis Center (CAC), U.S.A. with inputs from climate centres in Australia, Germany, the Russian Federation, Spain and the United Kingdom. The contributions were based, to a great extent, on the observational data collected and disseminated by the national Meteorological and Hydrological Services of the WMO Member countries.

Special appreciation is extended to Dr C. Ropelewski, Chairman of the WMO Commission for Climatology Working Group on Climate Change Detection, for his help in preparing the statement.

SUMMARY

In 1993, a number of climate anomalies and extreme events were reported over much of the globe. The major climate-influencing phenomenon that occurs in the tropical Pacific Ocean, commonly known as '*El Niño*/Southern Oscillation (ENSO)' continued to influence climate conditions in many areas in both the northern and southern hemispheres, particularly in the tropics. Elsewhere, there have been: droughts in parts of North America, Australia, Europe and South America; floods in North America and parts of Europe; and excessive warm spells and unusually cold outbreaks throughout the world. These events have brought considerable loss of life, much suffering and economic losses. However, there have also been benefits from some anomalies such as mild winter conditions.

The global surface mean annual air temperature for 1993 was about 0.2°C above the average for the 1951–1980 period. This positive global temperature anomaly (departure from normal) was lower than the peak value reached in 1990. The largest global land surface temperature anomalies occurred in the northern hemisphere. Considering the oceans, an extensive positive surface temperature anomaly over the central and eastern tropical Pacific, related to the ENSO, was the dominant feature.

Flooding, particularly in the central U.S.A., western Europe and in Asia, stands out among the anomalous precipitation-related events. During the 1992/1993 winter the northern hemisphere experienced its largest extent of seasonal snow cover since 1986. Significant anomalies in other components of the climate system included record low stratospheric ozone values over the Antarctic and low total ozone amounts over the northern hemisphere. Also, carbon dioxide measurements over the period 1991–1993 indicate that the growth rate has been well below that expected.

The variability in climate during 1993 may have been associated with climate change, but it is difficult to prove this linkage because of the lack of sufficient evidence and our incomplete understanding of the complex climate system. Therefore, care must be taken in attempting to relate the anomalies and their extent to climate change.

Surface temperatures

The estimated departures from normal (1951 to 1980) for the 1993 surface global mean temperature varied from +0.18°C to +0.24°C. These estimates vary, primarily because of slight differences in resolution, analysis, amount and distribution of data, although all estimates relied heavily on the 1993 land surface temperature data from the monthly CLIMAT messages exchanged over the Global Telecommunication System. Surface temperature data over the oceans were based on sea surface temperature measurements from ships. All of these estimated global surface temperature anomalies (departures from normal) were lower than the peak values reached in 1990 (Figure 1).

Based on surface land temperatures only (Figure 2) the mean annual tropical (20°N to 20°S) temperature anomalies have consistently averaged about +0.4°C during the past four years. Much of this warmth has been associated with the long-lived *El Niño*/Southern Oscillation (ENSO) episode in the tropical Pacific. In comparison, the 1993 extratropical land surface temperature anomaly was near +0.3 in the southern hemisphere and near +0.1 in the northern hemisphere.

In the southern hemisphere, the mean temperature anomaly pattern primarily reflected above-normal sea surface temperatures (SSTs) in the equatorial and subtropical Pacific Ocean and in the southwestern and south-central South Atlantic Ocean. Above-normal temperatures were also observed in South Africa and adjacent waters, and in east-central Australia.

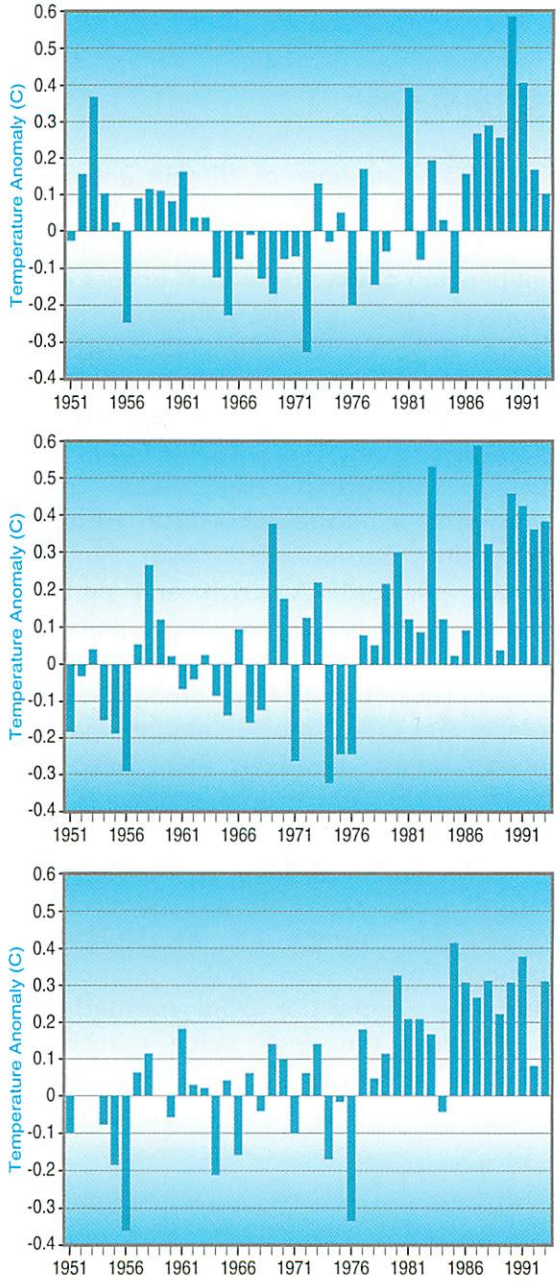

Figure 2
Annual estimated global (land only) surface temperature anomalies (°C) computed relative to the 1951–1980 base period for the northern hemisphere extratropics (top) tropics, (middle) and southern hemisphere extratropics (bottom).
Source: CAC

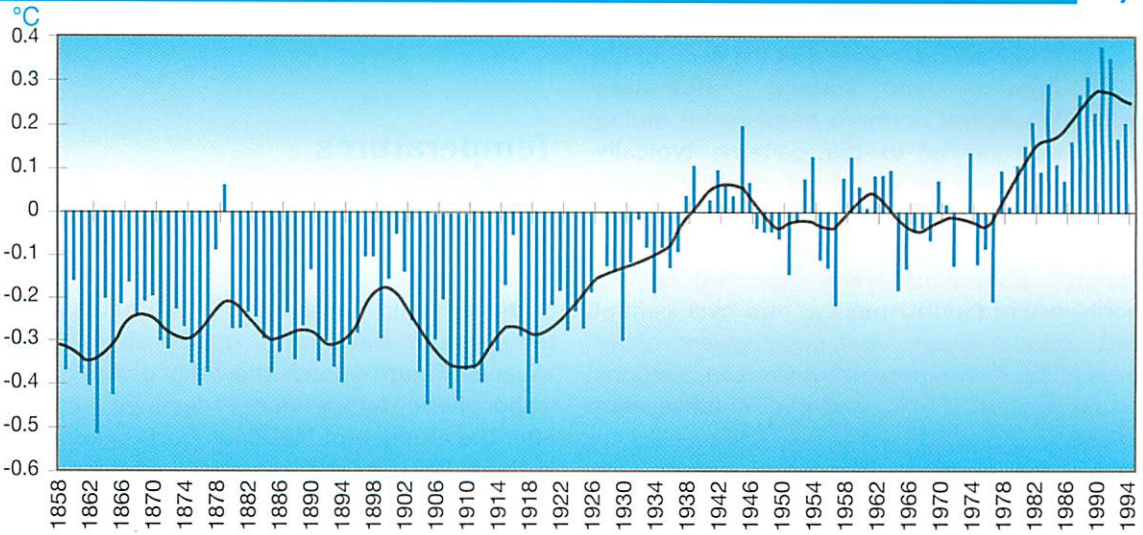

Figure 1
Global surface temperature anomalies are computed with respect to the 1951–1980 period. The graph is an update from the one used in the 1992 IPCC Supplement. Fitted curve is a 21-point binomial filter.
Source: Hadley Centre, Meteorological Office, U.K.

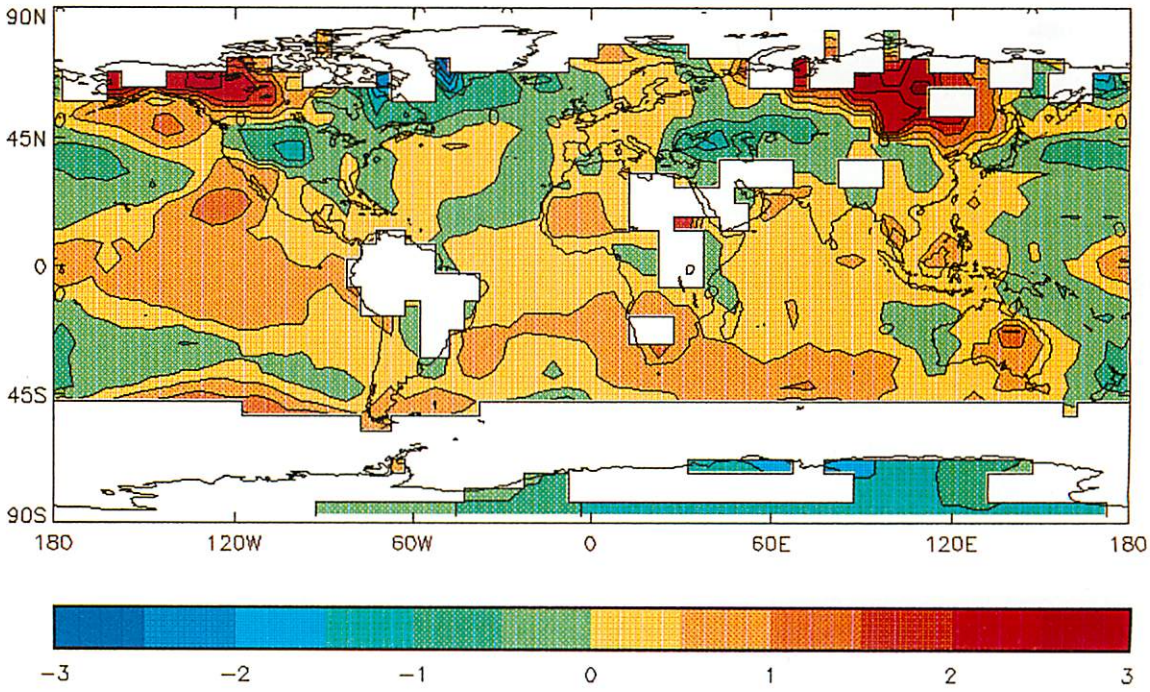

Figure 3
Surface temperature anomalies (°C) for January–December 1993. Analysis is based on at least 8 months of data. Areas with insufficient data are blank. Anomalies are computed relative to the 1951–1980 base period.
Source: Hadley Centre, U.K.

It is interesting to note that the geographic distribution of land surface temperature anomalies in the northern hemisphere during 1993 was similar to the patterns typically observed during the decade of the 1980's with the largest anomalies observed in the northern hemisphere. In Figure 3, it can be seen that positive anomalies were observed across northwestern North America, and over central and northern Russia, and negative anomalies were found over northeastern Canada, sections of the western U.S.A., and over southwestern Russia.

In the southern hemisphere extratropics (Figure 2, bottom), surface land temperature anomalies averaged +0.33°C during 1990 and 1991, but decreased to +0.09 in 1992, as volcanic aerosols from the eruption of Mt Pinatubo became dispersed throughout the hemisphere. As aerosol concentrations decreased during 1993, the temperature anomaly increased to approximately +0.3°C. In the northern hemisphere extratropics (Figure 2, top) a steady decrease in temperature occurred from 1990 through 1993, even though global stratospheric aerosols during 1993 decreased to levels observed prior to the eruption of Mt. Pinatubo.

Estimates of the 1993 global surface land temperature anomaly from all analyses were near 0.2°C, with a range of 0.18°C to 0.24°C. These anomalies are not significantly different from those estimated for 1992.

The extensive positive surface temperature anomaly over the central and eastern tropical Pacific, related to the ENSO was the dominant feature over the Oceans. Some less extensive negative anomalies occurred immediately to the north and south in the extratropical Pacific.

Temperatures in the atmosphere above the Earth's surface

Satellite-based temperature estimates and temperature data from upper air balloon ascents (Figure 4) both show that global mean tropospheric temperatures declined rapidly after the eruption of Mt. Pinatubo (Philippines) in June 1991, as the associated stratospheric aerosol cloud reflected a portion of the incoming solar radiation back towards space. The cooling trend subsided during the middle of 1992 and by the end of 1993 the mean global tropospheric temperature had risen to near the 1982–1991 base period mean.

In contrast, global mean lower stratospheric temperatures rose immediately after the eruption of Mt. Pinatubo (Figure 5). Temperatures subsequently peaked in September–October 1991 and declined steadily thereafter. By December 1993, global lower stratospheric temperatures reached the lowest values observed in the 15-year record from the NOAA-TIROS-N satellite microwave sounding unit. Lower than normal stratospheric temperatures in the tropical belt (30°S to 30°N) were the primary contributor to negative global stratospheric temperature anomalies.

The evolution of global-mean-stratospheric temperature anomalies are generally consistent with aerosol concentrations in the stratosphere. More radiation is absorbed and temperatures rise with higher aerosol concentrations and vice versa.

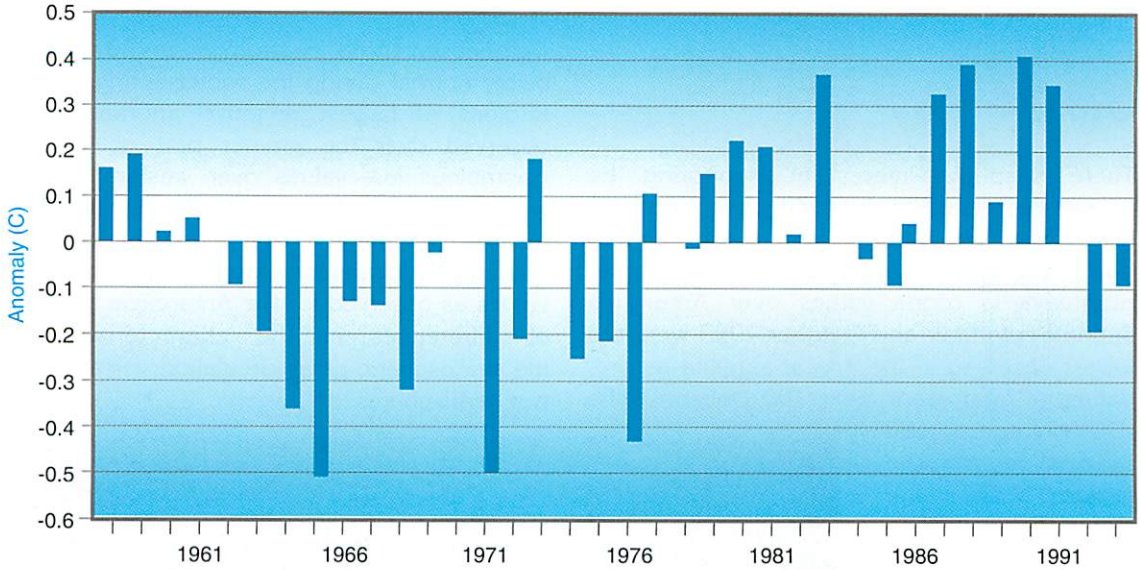

Figure 4
Annual global tropospheric (850–300 hPa) temperature anomalies derived from radiosonde data. Annual values of global tropospheric temperature anomalies are based on a 63-station network and were computed relative to the 1958–1991 base period.
Source: CAC (Data provided by J. Angell)

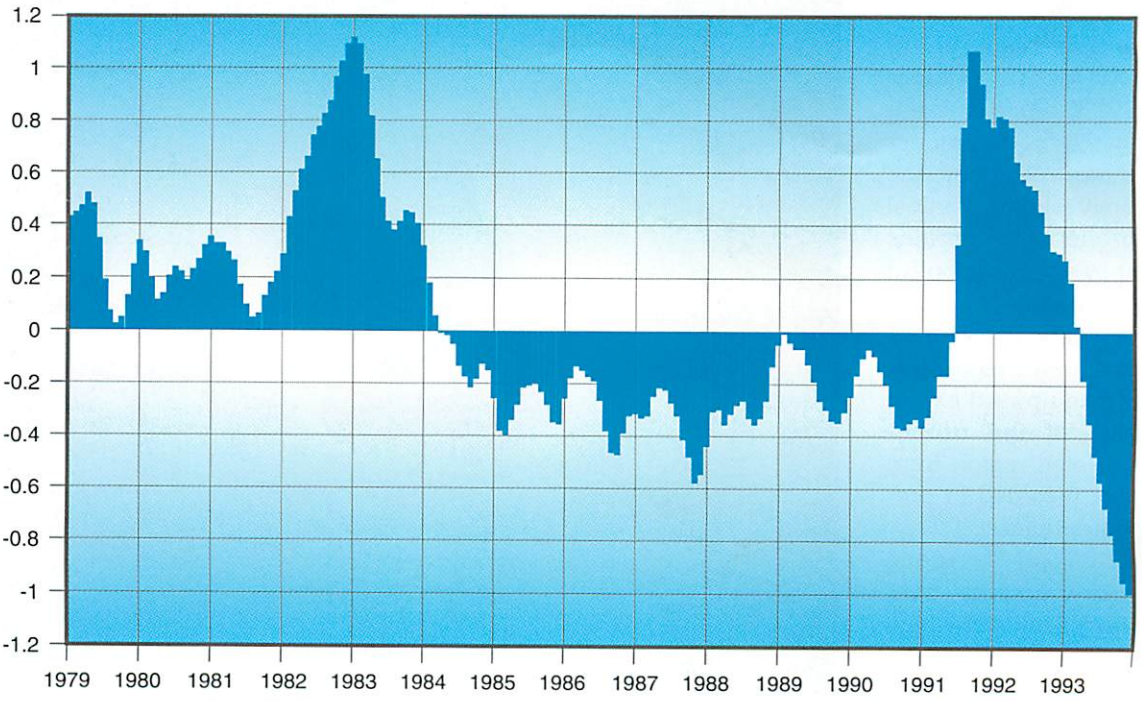

Figure 5
Lower stratospheric temperature anomalies from the Microwave Sounding Unit on the NOAA-TIROS-N polar orbiting satellite. Anomalies are computed relative to the 1982–1991 base period.
Source: CAC (Data provided by Spencer and Christy)

Ozone

There is special interest in monitoring the ozone over Antarctica during the southern hemisphere winter-spring seasons in connection with the Antarctic ozone hole. Stratospheric ozone values over Antarctica during September and October 1993 were the lowest observed in the 4-year satellite record. Values of total ozone near 100 Dobson Units (DU) were observed over a very large region of the Antarctic continent (Figure 6). A ground-based total ozone measurement of 96 DU for 12 October 1993, represents the lowest ozone amount measured over the South Pole. Vertical ozone profiles showed a region of complete ozone depletion between 14 to 19 km, representing an upward extension of the ozone-depleted region from that recorded in previous years.

Total ozone measurements over the middle and high latitudes of the northern hemisphere were observed to be from 9 to 20 percent below normal during the winter-spring period. Regions of largest negative anomaly were observed over the greater part of Europe. Anomalous low values over western Europe were typically observed to be in the 200 to 220 DU range. Ozone concentrations in the northern hemisphere do not reach such low values as observed for the Antarctica, because of differences in the characteristics of the stratospheric polar circulation vortex in the two hemispheres.

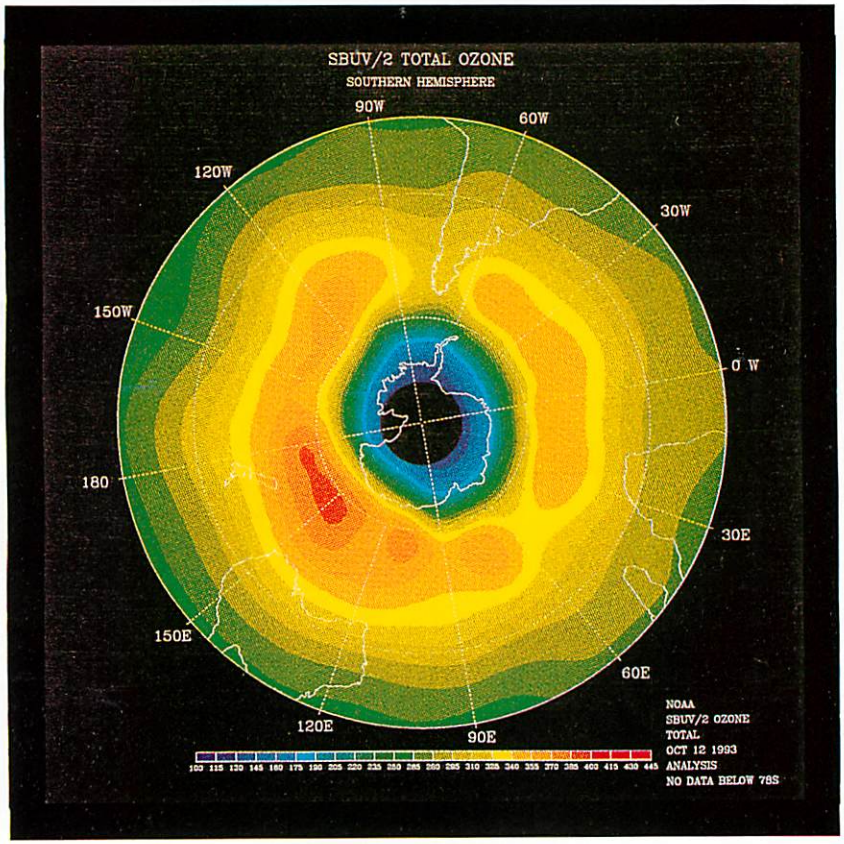

Figure 6
Southern hemisphere NOAA-11 SBUV/2 total ozone (DU) for 12 October 1993. Areas of lowest ozone are shown in blue and purple, with highest values in yellow and red. Regions of no data are shown in black.
Source: CAC

Aerosols

The Advanced Very High Resolution Radiometer (AVHRR) instrument on board the NOAA-11 polar-orbiting satellite provided data from which the atmosphere's aerosol optical thickness could be determined. Such observations were initiated two complete years before the Mt. Pinatubo eruption of June 1991. Weekly aerosol optical thickness differences from the weekly means of the two years (July 1989 through June 1991) have been monitored to study the added aerosol loading of the stratosphere due to the volcanic eruption.

As can be seen clearly in Figure 7, following the eruption of Mt. Pinatubo, the aerosol optical thickness differences initially showed a concentration of stratospheric aerosols over the tropics. In the months following the eruption, the differences showed the dispersal of the aerosols, first into the southern hemisphere then into the northern hemisphere. By March 1993, these differences were reduced to near zero. By June 1993, differences at most observable latitudes were virtually at zero. This does not mean that the stratosphere was entirely clean of aerosols created from the Mt. Pinatubo eruption. Rather, it indicates that, within the limitations of the observations from the AVHRR instrument, optical thicknesses in the entire atmosphere were at or below the same levels as those observed prior to the Mt. Pinatubo eruption.

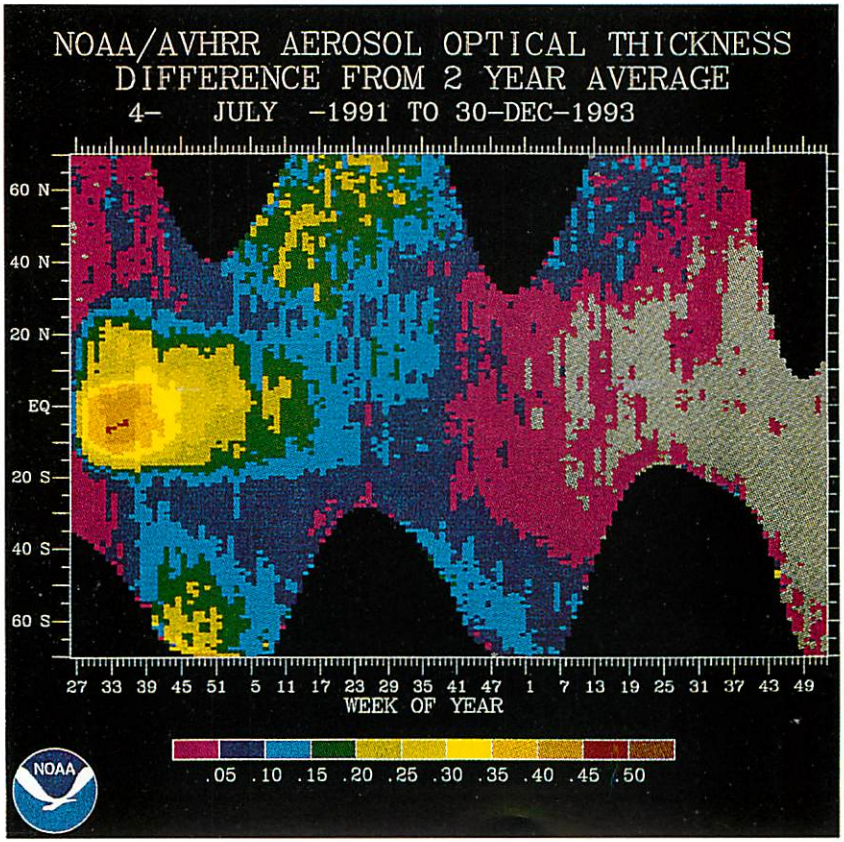

Figure 7
Weekly zonal averages of the aerosol optical thickness (AOT) from 70°S–70°N for the period 4 July 1991–30 December 1993. Differences are from the July 1989–June 1991 base period.
Source: CAC (Data provided by L. Stowe)

For more than 30 years, observations at Mauna Loa Observatory Hawaii have provided a measure of atmospheric aerosol concentrations. Figure 8 shows the effect of recent volcanic eruptions on aerosol concentrations over Mauna Loa. Following each eruption, the solar transmission ratio decreased as volcanic aerosol concentrations increased in the overlying atmosphere. Low transmission ratios continued for a longer period of time following the eruption of Mt. Pinatubo than for the period following the eruption of El Chichon. This is indicative of the larger overall global presence of aerosols injected into the atmosphere by Mt. Pinatubo.

Carbon dioxide and methane

Carbon dioxide is one of the most important gases thought to be associated with the enhanced greenhouse gas effect. It has been measured continuously at more than 30 WMO Global Atmosphere Watch observatories. The recent observational record over the period 1991–1993 indicates that the growth rate for carbon dioxide has been well below expectations. This reduced growth rate is evident in the lengthy record from the Mauna Loa Observatory in Hawaii which is a reliable indicator of large spatial scale long-term carbon dioxide growth (Figure 9). Similar features can be observed regarding the record of methane concentrations as shown in Figure 10.

Figure 9 (right) Monthly mean carbon dioxide concentrations (parts per billion) measured at Mauna Loa, Hawaii, 1957–1993. The data through 1973 are from C.D. Keeling at Scripps Institute of Oceanography.
Source: CAC (Data provided by NOAA/CMDL)

Figure 10 (right below) Globally averaged, biweekly methane mixing ratios in parts per billion by volume determined from the NOAA/CMDL Carbon Cycle Group cooperative air sampling network. Grey line shows the growth with the seasonal cycle removed.
Source: CAC

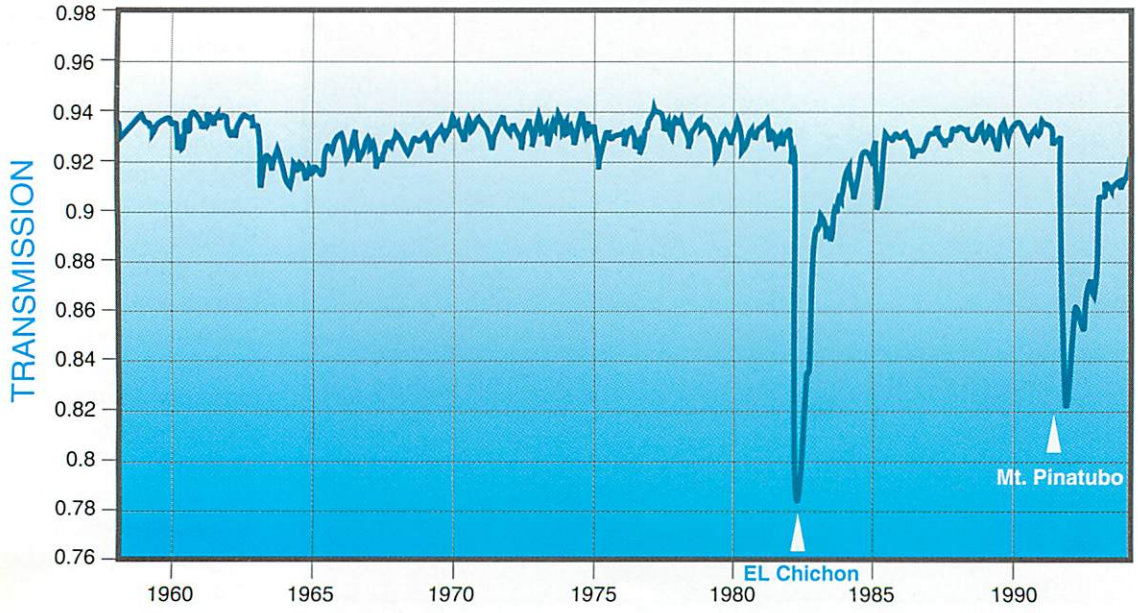

Figure 8 (left) "Apparent" atmospheric solar transmission at Mauna Loa Observatory, Hawaii as determined from direct solar radtion measurements.
Source: CAC (Data provided by E. Dutton)

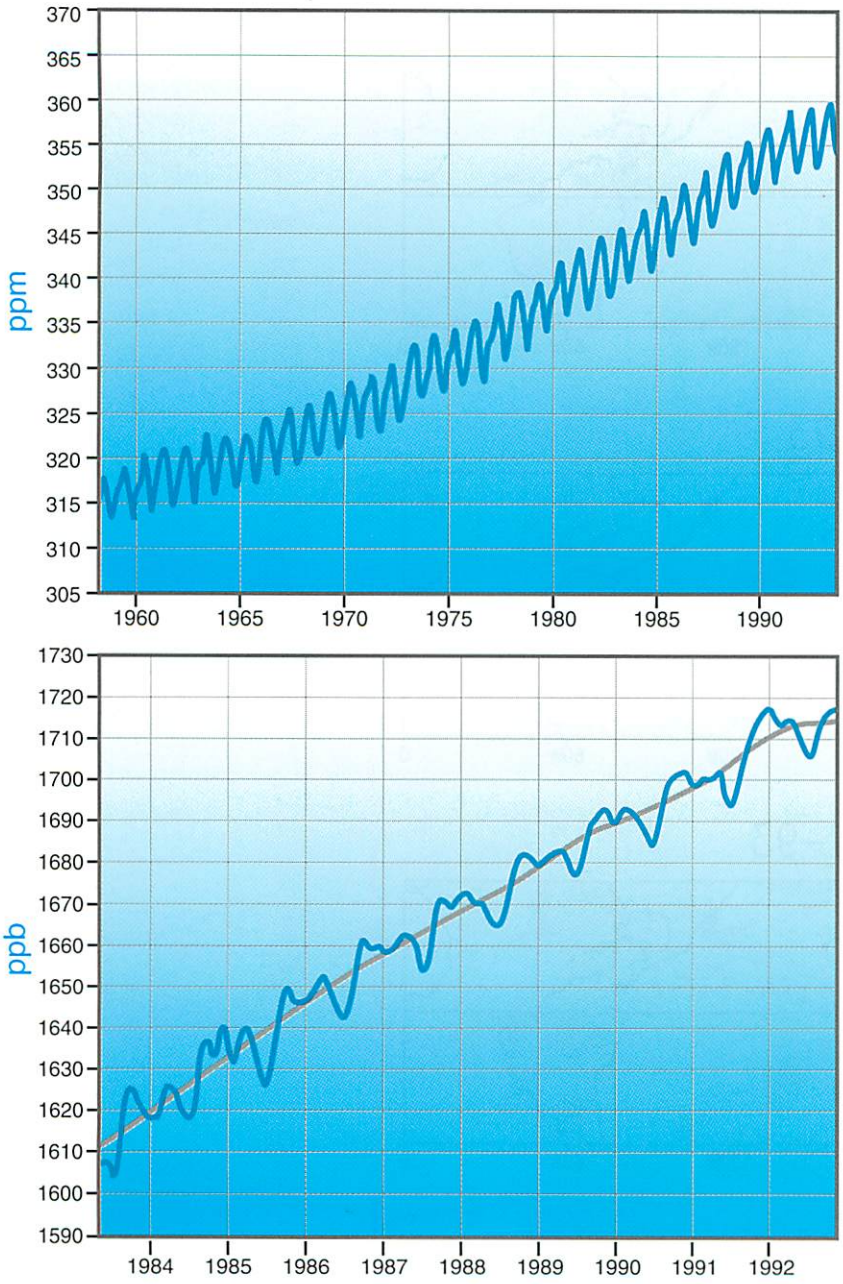

Unusually long-lived ENSO episode

Since 1990, the ENSO phenomenon has dominated the tropical Pacific Ocean. This current warm episode is the longest period of warm episode conditions in half a century, but it is not unprecedented. Extended warm episode-like conditions were also evident for the periods 1911–1913 and 1939–1942. Mature warm episode conditions first developed in late 1991. Positive sea surface temperature anomalies and enhanced convection dominated the central and eastern equatorial Pacific, accompanied by weaker than normal low-level easterly winds throughout the equatorial Pacific. Warm episode conditions redeveloped in early 1993 and continued until mid-1993. As in 1992, positive sea surface temperature anomalies persisted in the central equatorial Pacific during most of 1993, accompanied by enhanced convection.

Precipitation anomalies characteristic of warm episodes were observed in many areas. Estimated rainfall anomalies (1986–93 base period) reflect the warm episode conditions that were observed in the tropical Pacific during the year. Along the equator near the date line, monthly rainfall was estimated to be in excess of 150 mm above the 1986–93 normal during the period December 1992 through August 1993, while in the North Pacific Inter-Tropical Convergence Zone, rainfall was stronger than normal during March–May 1993. In contrast, below-normal rainfall occurred over Indonesia throughout the nine-month period and over northeast Brazil from March–August. Slightly weaker than

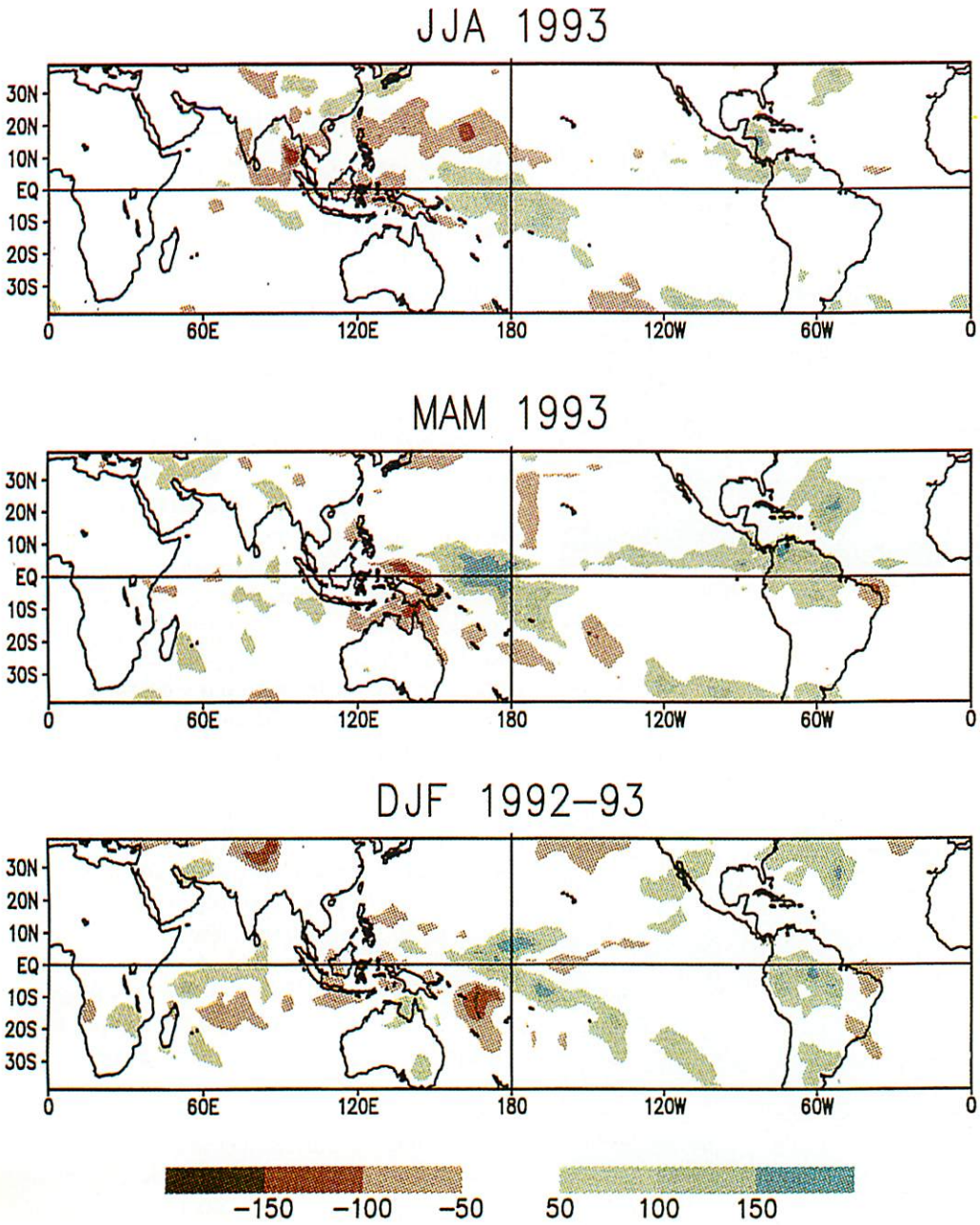

Figure 11
Satellite-derived rainfall anomaly estimates in mm/month. Anomalies are computed relative to the 1986–1993 base period.
Source: CAC

normal monsoon rainfall was also estimated for the region of western India. These rainfall anomaly features (Figure 11) are consistent with those observed during previous warm episodes.

Excessive rainfall, observed during early 1993 over California and other parts of the southwestern U.S.A. appears to be related, in part, to the pattern of warmer-than-normal sea surface temperatures in the central equatorial Pacific and the anomalous pattern of tropical cloudiness and precipitation that accompanied the unusually warm water.

By the end of 1993, warm episode conditions were steadily weakening throughout the tropical Pacific as the low-level equatorial easterly winds returned to near-normal intensity and the Southern Oscillation Index was near zero (Figure 12).

Cloudiness

One attempt to estimate global cloudiness has been conducted by Russian scientists based on derived data from visual and infrared images from the "Meteor" satellite system. The results have shown that mean cloud cover tends to be larger in the northern hemisphere (6.2 tenths) compared to the southern hemisphere (5.3 tenths). A time-series analysis of anomalous global cloudiness during the 28-year period 1966–1993 indicated an increase in global cloudiness during the first 20 years and a decrease in cloudiness after 1986. Global cloud cover during 1993 appeared to have increased slightly compared to 1992 values.

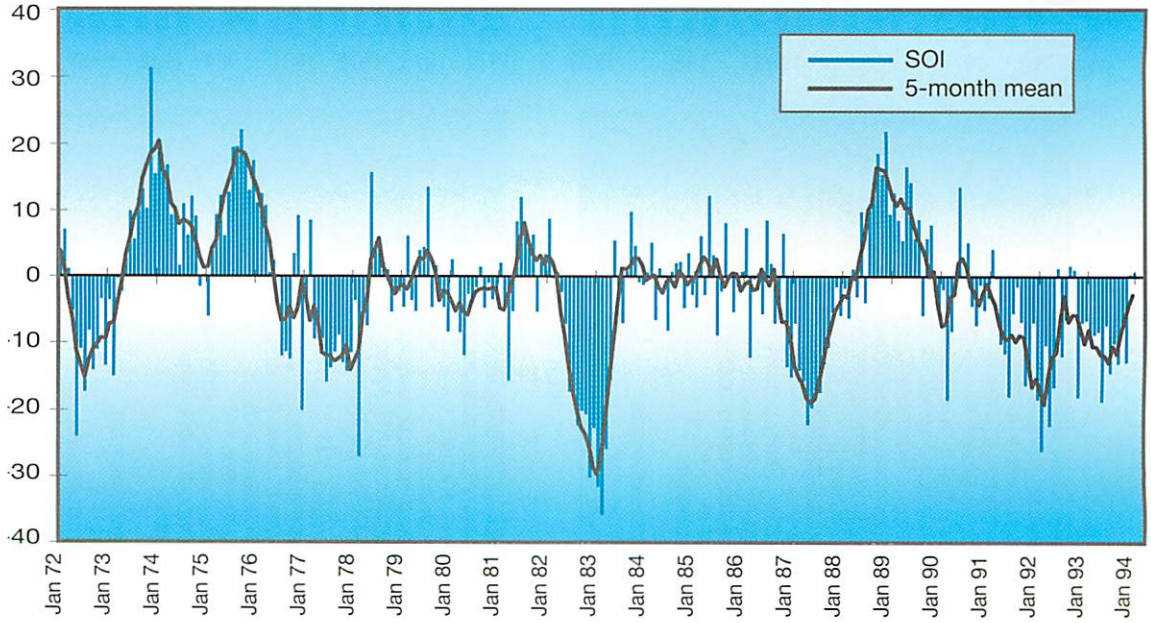

Figure 12
Time series of monthly values of SOI (difference between sea-level pressure anomalies at Tahiti & Darwin) standardized with repsect to mean monthly standard deviation. Solid curve shows 5 month running mean.
Source: Bureau of Meteorology, Australia

Snow and ice cover

During December 1992 through February 1993, the northern hemisphere experienced its largest extent of winter snow cover since 1986 (Figure 13). Snow cover was particularly heavy and persistent over western North America, Asia Minor and western Siberia.

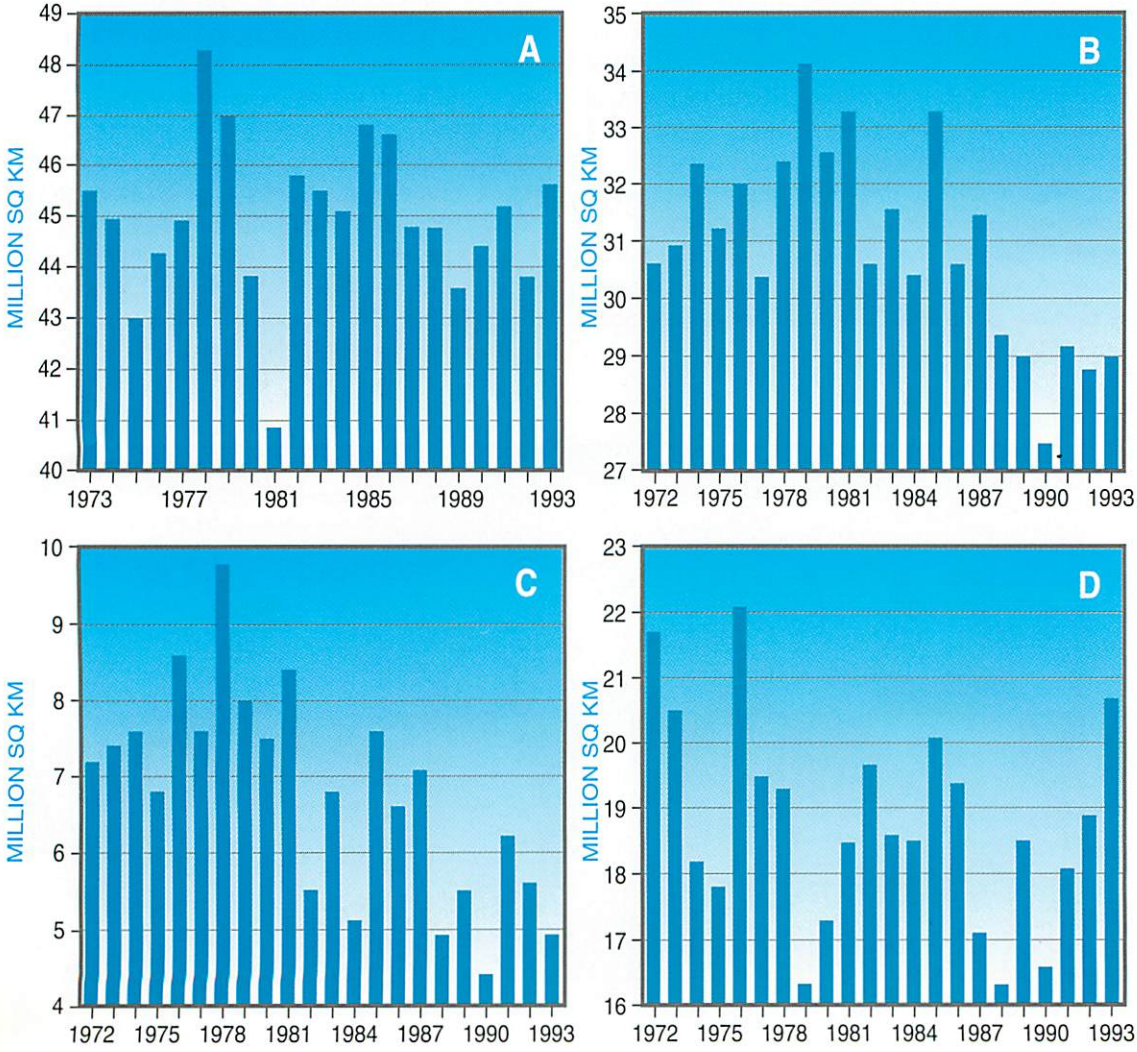

Figure 13
Time series of northern hemisphere snow-cover area (10^6 km^2) for (a) winter, December–February, (b) spring, March–May,(c) summer, June-August, (d) autumn, September–November; from satellite imagery.
Source: CAC (Data provided by NOAA/NESDIS and D. Robinson, Rutgers University)

Sea ice generally reaches its maximum extent during February in the northern hemisphere and during August in the southern hemisphere. In 1993, in both hemispheres, ice extent was above recent averages. In February in the Arctic it was above average for the first time since 1988 and in August the extent in the Antarctic (Figure 14) was above average for the first time since 1986. Time series analyses of both snow cover and ice cover back to 1973 show no clear evidence of systematic trends.

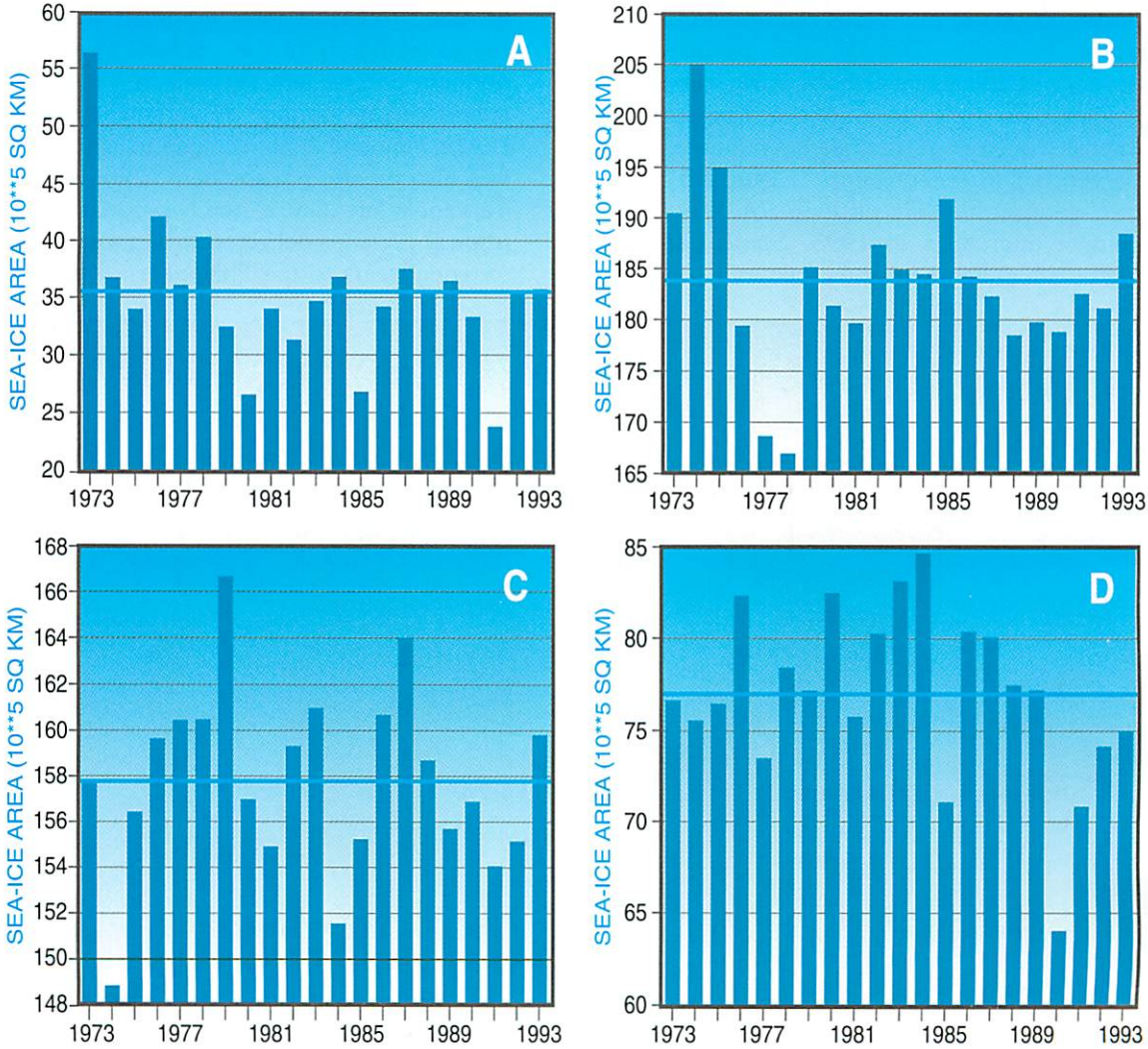

Figure 14
Time series of Antarctic sea ice (10^5 km^2) for (a) February, (b) August and Artic sea ice (c) February, (d) August. Solid line depicts the 1973–1993 mean
Source: CAC

EXTREME AND ANOMALOUS CLIMATE EVENTS IN 1993

A number of extreme climate events, notably floods, occurred in various regions around the world in 1993. Despite the number and severity of the events, there is no conclusive evidence to indicate that the frequency or intensity of such events has been increasing or decreasing in recent years. Figure 15 shows the geographic distribution of the major climate anomalies in 1993. Some particular regional highlights were as follows:

- In **Africa**, torrential downpours in Zimbabwe, northern Mozambique, most of Malawi, Tanzania, and Kenya during the first few months of the year continued to alleviate drought conditions which afflicted the area in 1991 and much of 1992, but also engendered localized flooding.
- In **Asia**, excessive rains triggered some of the worst floods of the century along the northern and eastern sections of the Indian subcontinent during July and August. During May and June, considerable flooding was also reported in southern China and in Taiwan. In late July, a steady progression of tropical cyclones delivered strong winds and torrential rains to the Philippines, Vietnam,

Figure 16
Precipitation (mm): total (top) and anomalous (bottom) during June–August 1993. Anomalies are computed relative to 1961–1990.
Source: CAC

Figure 15
Significant climate anomalies and episodic events during 1993.
Source: CAC

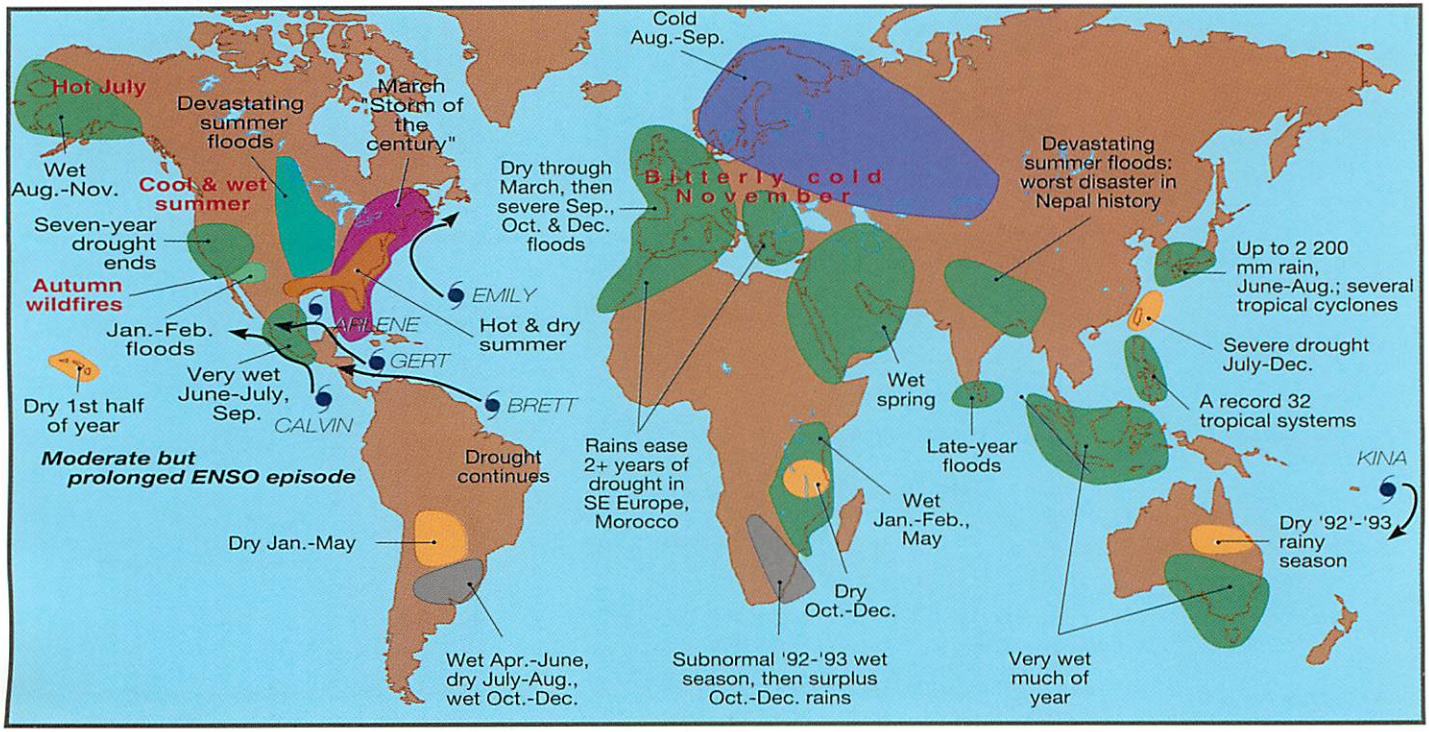

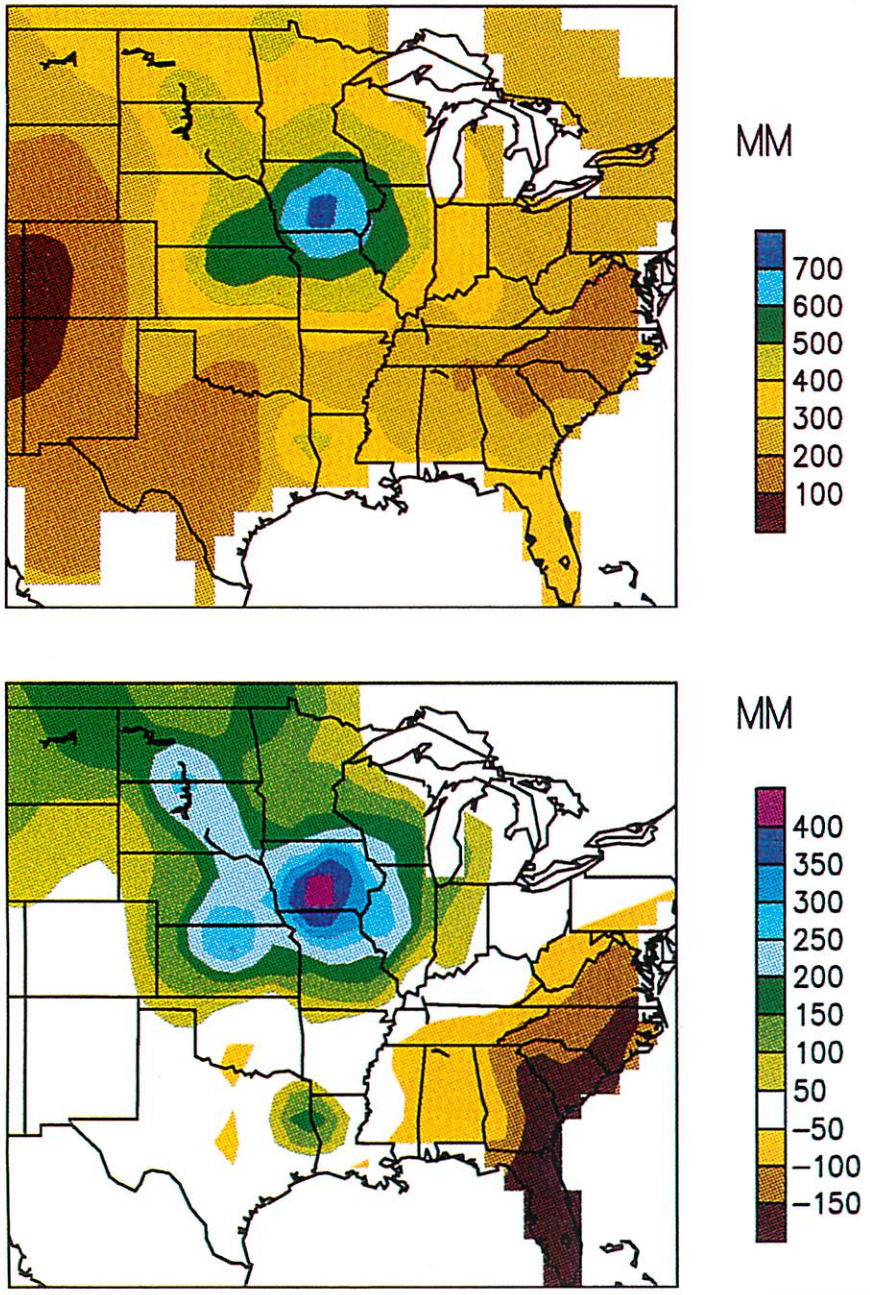

and southern China. During November, a vigorous northeast monsoon produced extreme precipitation and flooding over southern India and northeastern Sri Lanka. The Philippines were affected by 32 tropical systems during 1993 (the most on record for a single year).

- In **South America**, much wetter than normal conditions occurred during the first part of the year in Uruguay, southern Brazil and portions of northern Argentina; a rainfall pattern consistent with the continued occurrence of the *El Niño*/Southern Oscillation (ENSO) episode. Three times the normal rainfall was observed in eastern Argentina and Uruguay for the period April through mid-May. Generally wetter than normal conditions were also observed in Ecuador and northern Peru with mature ENSO conditions.
- In **North America** during the winter of 1992/1993, significant above-normal precipitation finally fell throughout California, alleviating the long-term drought conditions. The midwestern U.S.A. experienced one of its worst flooding events on record during June–July 1993 (Figure 16). The region of extensive flooding encompassed nine states, including most of the central basin of the U.S.A. According to the United States Geological Survey (USGS), the magnitude of the damages from the floods in terms of property damage, disrupted business, and personal trauma was unmatched in United States history.
- In **Australia**, drought conditions became entrenched over northeastern Australia, with unprecedented long-term rainfall deficiencies in some areas. Heavy rains and

serious flooding over the southeast were a feature of the spring. Rainfall totals from early October to mid-December were between two and five times the normal amount in parts of South Australia, New South Wales, and Victoria.

- In **Europe**, more than 300 mm of precipitation was recorded over much of the continent during the September to December period. A monthly record 192 mm of precipitation was recorded in Madrid, Spain in October. The largest precipitation totals, over 500 mm, fell in the Black Forest of southern Germany (Figure 17) and in Swiss Alps where incidents of severe flooding occurred in some valleys. In early December, strong storms pounded Europe with 145 km/h wind gusts and torrential rains, generating the worst flooding in 60 years across parts of France, the Benelux countries, and Germany. Further east, record cold temperatures gripped large portions of Europe, Scandinavia and western Asia from September to November with mean monthly surface air temperatures over this period 3–4°C below normal throughout much of Scandinavia and Russia.

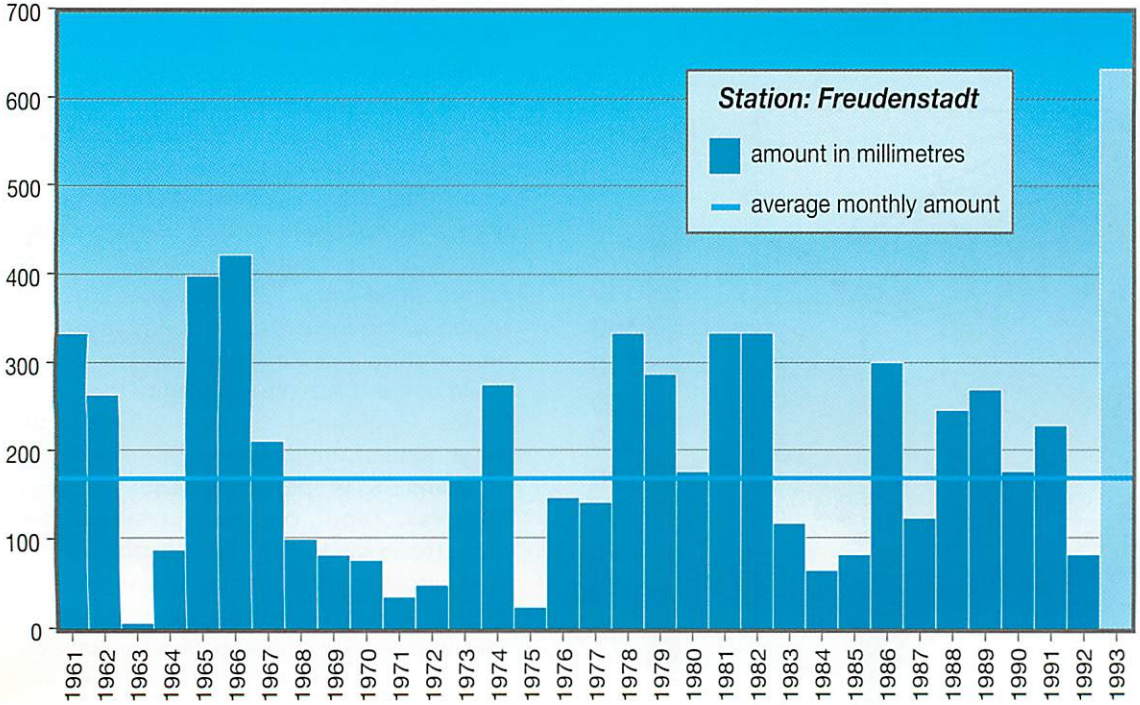

Figure 17
Monthly amount of precipitation (December)
Source: Deutscher Wetterdienst, Germany